USGS
science for a changing world

National Assessment of Hurricane-Induced Coastal Erosion Hazards: Gulf of Mexico

By Hilary F. Stockdon, Kara J. Doran, David M. Thompson, Kristin L. Sopkin, Nathaniel G. Plant, and Asbury H. Sallenger

Open-File Report 2012–1084

U.S. Department of the Interior
U.S. Geological Survey

U.S. Department of the Interior
KEN SALAZAR, Secretary

U.S. Geological Survey
Marcia McNutt, Director

U.S. Geological Survey, Reston, Virginia 2012

This report and any updates to it are available online at:
http://pubs.usgs.gov/of/2012/1084/

For more information on the USGS—the Federal source for science about the Earth,
its natural and living resources, natural hazards, and the environment:- visit http://www.usgs.gov
or call 1-888-ASK-USGS

For an overview of USGS information products, including maps, imagery, and publications,
visit *http://www.usgs.gov/pubprod*

To order this and other USGS information products, visit *http://store.usgs.gov*

Suggested citation:
Stockdon, H.F., Doran, K.J., Thompson, D.M., Sopkin, K.L., Plant, N.G., and Sallenger, A.H., 2012, National assessment of hurricane-induced coastal erosion hazards: Gulf of Mexico: U.S. Geological Survey Open-File Report 2012-1084, 51 p.

Contents

Figures

Tables

Conversion Factors

SI to Inch/Pound

Multiply	By	To obtain
	Length	
centimeter (cm)	0.3937	inch (in.)
millimeter (mm)	0.03937	inch (in.)
meter (m)	3.281	foot (ft)
kilometer (km)	0.6214	mile (mi)
kilometer (km)	0.5400	mile, nautical (nmi)
meter (m)	1.094	yard (yd)
	Flow rate	
meters per second (m/s)	2..237	mile per hour (mi/h)

Vertical coordinate information is referenced to North American Vertical Datum of 1988 (NAVD 88)

Horizontal coordinate information is referenced to the North American Datum of 1983 (NAD 83)

Additional Abbreviations and Acronyms

ACRONYM OR ABBREVIATION	DEFINITION
CHARTS	Compact Hydrographic Airborne Rapid Total Survey
DEM	Digital Elevation Model
EAARL	Experimental Advanced Airborne Research Lidar
GPS	Global Positioning System
HWL	High Water Line
Hz	Hertz
IPCC	Intergovernmental Panel on Climate Change
Lidar	Light Detection and Ranging
MHW	Mean High Water
MOM	Maximum of the Maximum
NAD83	North American Datum 1983

NAVD88	North American Vertical Datum 1988
NGVD29	National Geodetic Vertical Datum 1929
NHC	National Hurricane Center
NOAA	National Oceanic and Atmospheric Administration
RMS	Root-Mean-Square
SLOSH	Sea, Lake, and Overland Surges from Hurricanes
SWAN	Simulating WAves Nearshore
USACE	U.S. Army Corps of Engineers
USGS	U.S. Geological Survey
WIS	Wave Information Studies

National Assessment of Hurricane-Induced Coastal Erosion Hazards: Gulf of Mexico

By Hilary F. Stockdon, Kara S. Doran, David M. Thompson, Kristin L. Sopkin, Nathaniel G. Plant, and Asbury H. Sallenger

1. Introduction

1.1 Impacts of hurricanes on coastal communities

Beaches serve as a natural barrier between the ocean and inland communities, ecosystems, and natural resources. However, these dynamic environments move and change in response to winds, waves, and currents. During extreme storms, such as powerful hurricanes, changes to beaches can be large, and the results are sometimes catastrophic. Lives may be lost, communities destroyed, and millions of dollars spent on rebuilding.

During storms, large waves may erode beaches, and high storm surge shifts the erosive force of the waves higher on the beach. In some cases, the combined effects of waves and surge may cause overwash or flooding. Structures built on or a near a dune can be undermined during wave attack and subsequent erosion. During Hurricane Ivan in 2004, a five-story condominium in Orange Beach, Ala., collapsed after the sand dune supporting the foundation eroded (fig. 1).

Figure 1. A five-story condominium in Orange Beach, Alabama, collapsed when the dune underlying its foundation was eroded during the September 2004 landfall of Hurricane Ivan.

Waves overtopping a dune can transport sand inland, covering roads and blocking evacuation routes or emergency relief (fig. 2). If storm surge inundates barrier island dunes, currents flowing across the island can create a breach, or new inlet, completely severing evacuation routes. Waves and surge during the 2003 landfall of Hurricane Isabel left a 200-meter (m) wide breach that cut the only road to and from the village of Hatteras, N.C. (fig. 3).

Figure 2. Waves and surge left an overwash deposit covering the road in Pensacola Beach, Florida, after Hurricane Ivan in September 2004 (photo credit: Jeff Lillycrop, U.S. Army Corps of Engineers).

Extreme coastal changes caused by hurricanes may increase the vulnerability of communities both during a storm and to future storms. For example, when sand dunes on a barrier island are eroded substantially, inland structures are exposed to storm surge and waves. Absent or low dunes also allow water to flow inland across the island, potentially increasing storm surge in the back bay and on the mainland. During Hurricane Isabel the protective sand dunes near the breach were completely eroded, increasing vulnerability to future storms (fig. 4).

Figure 3. Storm surge, waves, and currents from Hurricane Isabel (August 2003) cut a breach across Highway 12, on Hatteras Island, North Carolina, severing the single road in and out of the village. The Atlantic Ocean is located to the left of the image. Asphalt from the highway is on the right side of the image. See figure 4 for aerial view of breach.

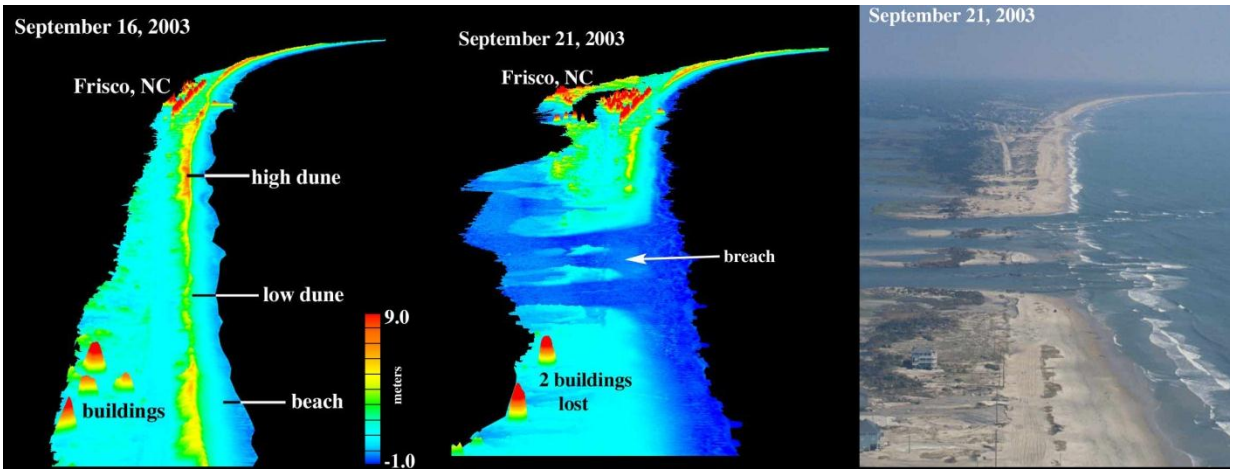

Figure 4. Lidar-based elevations of Hatteras Island, North Carolina, before (left) and after (middle) the landfall of Hurricane Isabel in September 2003 show erosion of the seaward-most dune and subsequent breaching (right). See figure 3 for a ground view of the breach. Note: lidar surveys did not cover the same, or full, width of island during each survey.

1.2 Prediction of hurricane-induced coastal erosion

In the last decade, gulf coast communities have been devastated by many powerful hurricanes including Charley (2004), Ivan (2004), Katrina (2005), Rita (2005), and Ike (2008). Waves and surge accompanying these storms resulted in widespread beach and dune erosion and extensive overwash (Sallenger and others, 2006; Doran and others, 2009a; Doran and others, 2009b). There exists a clear need to identify areas of our coastline that are likely to experience extreme erosion during a hurricane. This information can be used to determine vulnerability levels associated with building houses or infrastructure on land that shifts and moves with each storm landfall. A decade of research on storm-driven coastal change hazards within the U.S. Geological Survey (USGS) National Assessment of Coastal Change Hazards project has provided the data and modeling capabilities to produce the first regional assessment of the vulnerability of coastlines to extreme erosion during hurricane landfall. Vulnerability is defined in terms of the probability for coastal change, predicted using a USGS-developed storm-impact scale that compares predicted elevations of hurricane-induced water levels to measured elevations of coastal topography (Sallenger, 2000). This approach defines four coastal change regimes that describe the dominant interactions between beach morphology and storm processes and resulting modes of coastal change. Here, we focus on the sandy beaches on the U.S. Gulf of Mexico coastline. These beaches are among the most vulnerable in the Nation due to low coastal elevations and frequent hurricane landfalls.

1.3 Storm-scaling model

During a storm, the combined effects of (1) the astronomical tide, (2) storm surge, and (3) wave runup (both setup, η_{setup}, and swash, S) move the erosive forces of the storm higher on the beach than during typical wave conditions. The total elevation of these three parameters defines two key metrics

that characterize the nearshore hydrodynamic forcing of a storm: (1) the extreme high water level attained during a storm, defined here as the 98-percent exceedance level (η_{98}), and (2) the storm-induced mean water level (η_{50}), defined by only storm surge, tide, and wave setup.

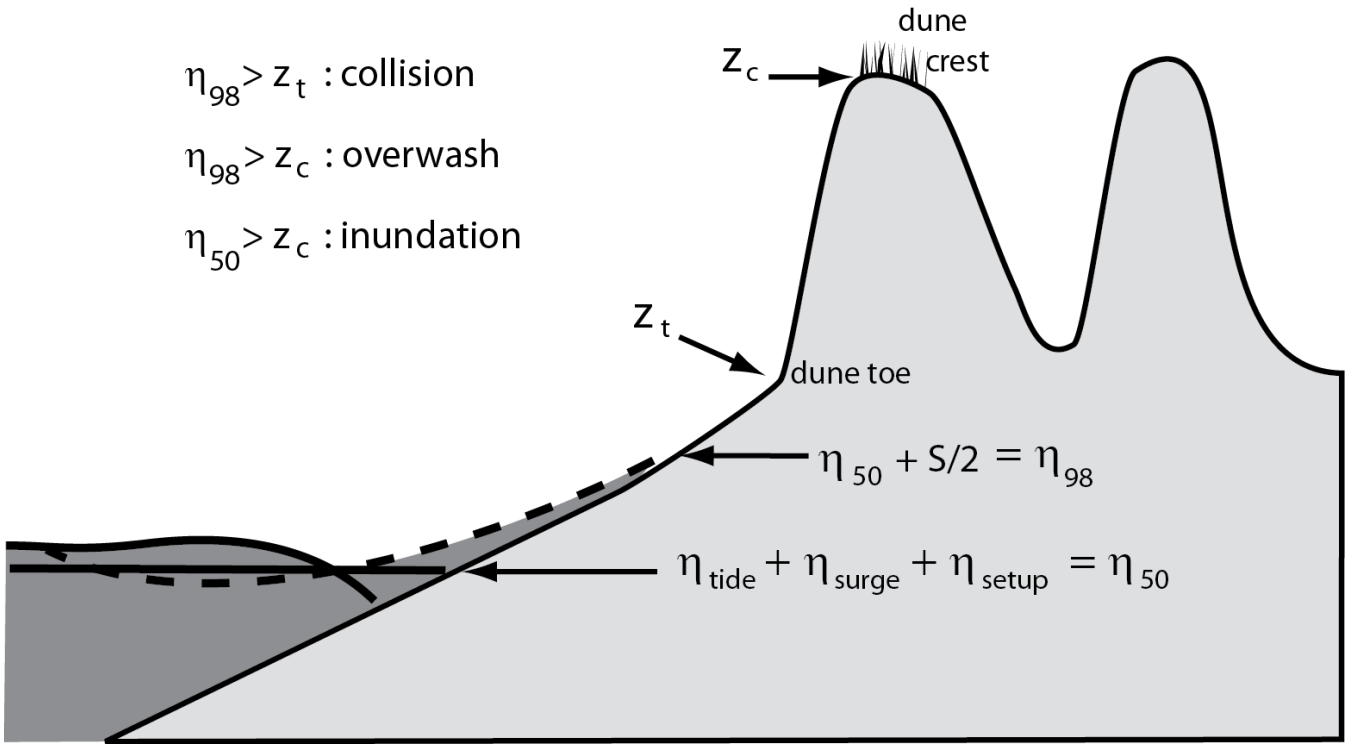

Figure 5. Sketch defining the relevant morphologic and hydrodynamic parameters in the storm impact scaling model of Sallenger (2000) (modified from Stockdon and others, 2009).

Water level elevations are compared to the elevation of the toe (z_t) and crest (z_c) of the most seaward sand dunes that define the landward limits of the beach system and represent the first-line defense of a barrier island to an approaching storm. Using these parameters, four storm-impact regimes, or thresholds for coastal change, are defined to provide a framework for examining the general types and relative magnitudes of coastal change that are likely to occur during hurricanes (fig. 5) (Sallenger, 2000; Stockdon and others, 2007a).

- *swash* ($\eta_{98} < z_t$)
- *collision* ($\eta_{98} > z_t$)
- *overwash* ($\eta_{98} > z_c$)
- *inundation* ($\eta_{50} > z_c$)

(Note: Following Plant and Stockdon (in press), our nomenclature differs from Sallenger (2000) to emphasize probabilistic definition of water levels and to clearly distinguish both the horizontal and vertical components of dune morphology.)

Figure 6. Examples of collision (Nags Head, North Carolina; Isabel, 2003), overwash (Santa Rosa Island, Florida; Ivan, 2004), and inundation (Dauphin Island, Alabama; Katrina, 2005).

The *swash* regime represents a range of relatively calm weather conditions, where water levels are confined to areas seaward of the dune base. Sand that is eroded from the beach during more energetic periods is transported offshore and will return to the beach during more quiescent conditions. The erosion and recovery cycle can occur over a time span on the order of weeks. When waves reach the base of the dune (*collision* regime), the front of the dune is expected to erode (fig. 6, left). Again, sand is transported seaward and then re-deposited on the beach or sandbar or transported alongshore. In

this case, the beach is likely to recover in the weeks and months following the storm. However, because aeolian processes are responsible for natural dune growth, recovery of the dune may take years.

In more extreme cases, such as during stronger storms and for relatively lower dunes, waves and surge may exceed the dune crest elevation, resulting in *overwash*. Under these conditions, waves transport sand landward from the beach and dune (fig. 6, center). Impacts may be more long-lasting, or even permanent, in this regime as sand is deposited inland, making it unavailable for natural recovery following a storm. During *inundation* of the beach (fig. 6, right), storm-induced mean water levels exceed the elevation of the crest of the primary dune or berm. Within this regime some of the most extreme coastal changes occur on barrier islands: the beach system (dune crest and beach) is completely submerged, and net landward transport of sediment is likely to occur (Sallenger, 2000). Typically, larger magnitudes of shoreline retreat and beach erosion will occur when the beach is inundated due to transport of sand occurring under all storm scale regimes (Stockdon and others, 2007a). On narrow barrier islands, inundation allows strong currents to cross the island and focus where dunes are low, carving breaches.

The predictive accuracy of the storm-impact scaling model was tested by hindcasting the likely impact of Hurricanes Bonnie (1998) and Floyd (1999) (Stockdon and others, 2007a) and of Hurricane Ivan (2004) (Stockdon and others, 2007b) and comparing this with observed morphologic changes. For Hurricane Ivan, the overall hindcast accuracy of the model in predicting one of the four regime types was 68 percent. The accuracy of the model varied between regimes and was highest for the overwash conditions. Underprediction of the actual storm response was more likely than over prediction. Errors were likely due to profile evolution of the low-lying barriers during the storm. As dune-crest elevation was lowered, the collision regime could proceed to overwash and then inundation.

With skillful hindcasting results, the model has also been applied in real time for landfalling hurricanes (Plant and others, 2010). Using pre-storm measurements of dune elevations and real-time forecasts of storm surge and wave conditions, the USGS routinely reports the likelihood of beaches experiencing coastal change associated with collision, overwash, and inundation. These analyses are posted online (*http://coastal.er.usgs.gov/hurricanes*) and revised with updated hydrodynamic forecasts as the storm makes landfall.

Using a similar methodology, this report quantifies the likely impact of a hypothetical hurricane landfall on the Gulf of Mexico coastline. The probabilities of hurricane-induced coastal change are used to define the vulnerability of this region to extreme erosion from waves and storm surge associated with category 1-5 hurricanes.

2. Methods

In order to use this model for a large-scale assessment of the potential for coastal change during future hurricane landfall, accurate estimates of (1) the dune parameters and (2) the expected hurricane-induced water level for hypothetical storms are needed. Well documented models of storm surge have been used to estimate worst-case scenarios of water level elevations for category 1-5 hurricanes and can be used directly by our modeling approach. Simulations of corresponding wave conditions for category 1-5 hurricane landfalls are more challenging, but given simplifying assumptions it is possible to determine worst-case scenario wave heights for each category. Numerical simulations of storm surge and wave heights support application of our approach to large stretches of coast. Lidar topographic surveying has made it possible to accurately measure dune elevations along long (hundreds of kilometers) stretches of coastline. The combination of high-resolution measurements and advanced

hydrodynamic modeling makes it possible to estimate probabilities of hurricane-induced coastal change and to identify coastal erosion vulnerability at a national scale.

2.1 Lidar-derived beach morphology

The morphology of the beaches and dunes was mapped using airborne lidar topographic surveys conducted from 2000 to 2008 by the U.S. Army Corps of Engineers (USACE) Compact Hydrographic Airborne Rapid Total Survey (CHARTS) and the USGS Experimental Advanced Airborne Research Lidar (EAARL) systems. The combination of laser-based ranging and GPS-based navigation provides an efficient method for collecting high-resolution data of sub-aerial topography with sufficient accuracy (Root-Mean-Square (RMS) vertical accuracy = 15 centimeters, cm) to resolve the spatial details of sand-dune elevation and position (Sallenger and others, 2003). Three-dimensional lidar data were gridded using a fixed-scale interpolator (Plant and others, 2002), which allows for variability in cross-shore and alongshore resolution, here, 2.5 m and 10 m, respectively. In addition to a gridded topographic surface, this method produces a corresponding grid of the RMS error, which provides a measure of noise in the data. A Hanning filter with a width equal to two times the grid resolution was chosen to minimize noise in the data associated with vegetation, alongshore variability, and other error sources while preserving distinct morphology. Analysis of cross-shore profiles of gridded data allows for automated extraction of dune crest and toe, as well as shoreline position and beach slope, at a regular alongshore interval, here, 10 m (fig. 7). These features are ultimately used to estimate wave runup and the corresponding storm-response regimes, as well as to measure actual morphologic changes before and after storms.

2.1.1 Shoreline position

Shoreline position (x_{sl}) is defined as the horizontal location of the intersection of mean-high water (MHW) contour with the beach profile. The elevation of MHW around the Gulf of Mexico was defined using long-term observations from open-coast tide gages (Weber and others, 2005). The cross-shore location of the MHW shoreline was automatically extracted from gridded lidar data using a probabilistic approach that makes use of the RMS error surface, providing for a statistically robust estimate. The probability that each gridded elevation was equal to the local MHW value was computed from a normal distribution of the beach elevation, using the interpolated elevation as the mean (μ) and the lidar scatter (noise) as the standard deviation (σ). Using a prior shoreline as a first approximation, the grid cell with the highest probability within a defined distance (3 times the standard deviation of all shoreline points within the grid segment) of the prior shoreline was selected as the most likely shoreline. A linear regression using the selected point and adjacent grid cells was used to identify a more precise cross-shore location of the MHW line. The confidence interval on the estimate was defined from the regression error and the error on lidar data.

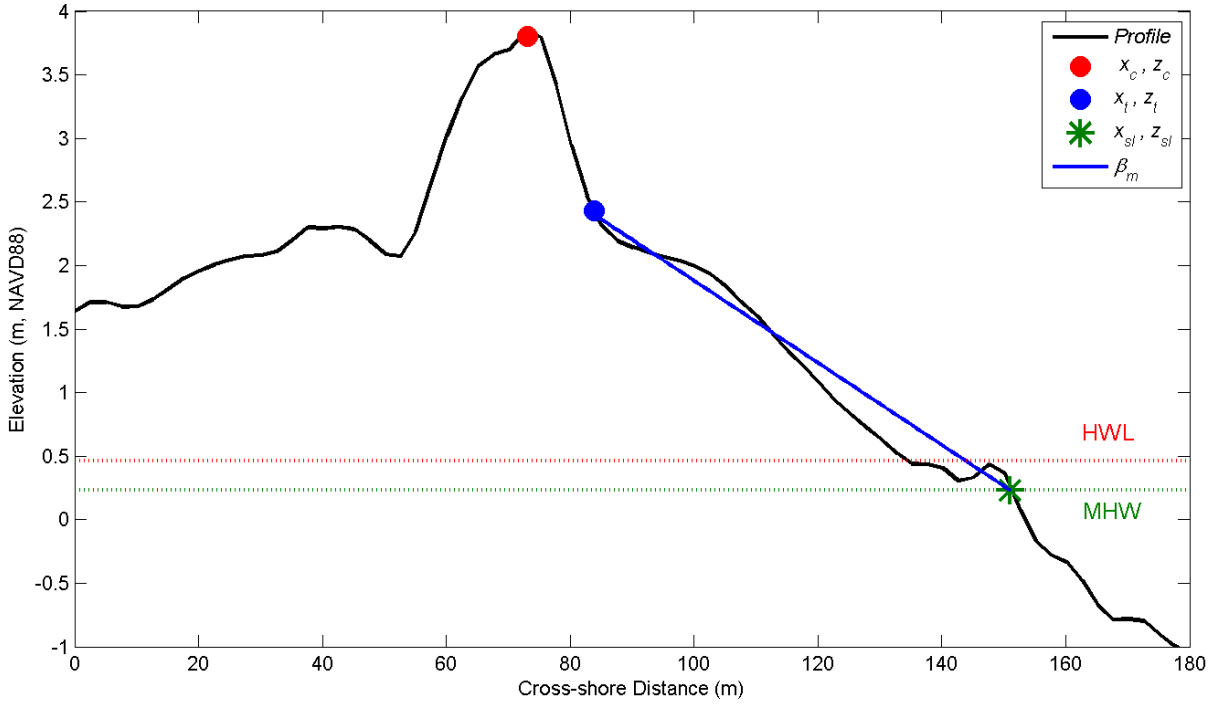

Figure 7. Cross-shore profile of lidar-based elevations indicating the locations of the dune crest (x_c, z_c), toe (x_t, z_t), shoreline (x_{sl},z_{sl}), mean beach slope (β_m), mean high water (MHW), and high water line (HWL). Abbreviation: m, meter.

2.1.2 Dune Crest

For this analysis, the seaward-most sand dune at any location along the coast defines the landward limit of the beach system. The position and elevation (x_c,z_c) of the dune crest or, in the absence of a dune, the beach berm were extracted every 10 m along the coast from cross-shore profiles of gridded lidar topography (fig. 7). An automatic algorithm was used to select the peak of the most seaward dune along each cross-shore profile (Stockdon and others, 2009). The approach is based on finding inflection points in the cross-shore slope, computed across a sliding 5-m window, and classifying them as morphologic crests and troughs. The highest crest elevation was identified as the crest of the primary dune. Several quality control checks ensure that an appropriate dune/berm location was selected. Dune/berm selection is restricted to locations where:

- x_c is within 200 m of the shoreline,
- x_c is seaward of built structures, identified as locations where local slope exceeds a threshold limit of 34°,
- RMS error on z_c is less than 0.5 m, a pre-defined noise tolerance, and
- z_c is higher than the MHW elevation.

The results of the automated analysis were checked to verify that an alongshore coherent dune feature was identified and that it was located seaward of coastal structures and roads. ArcGIS shapefiles of dune peaks generated from the two-dimensional cross-shore profiles during the automated process were viewed in combination with the three-dimensional gridded lidar dataset (fig. 8) and GoogleEarth images. In regions of complex topography, this step ensured that regions of steep topography such as escarpments were not erroneously labeled as buildings. When inconsistencies were found, the algorithm was re-initialized, and the results were viewed in a graphical user interface that displayed interpolated and point cloud lidar data. Errors were corrected by removing or editing dune crest positions.

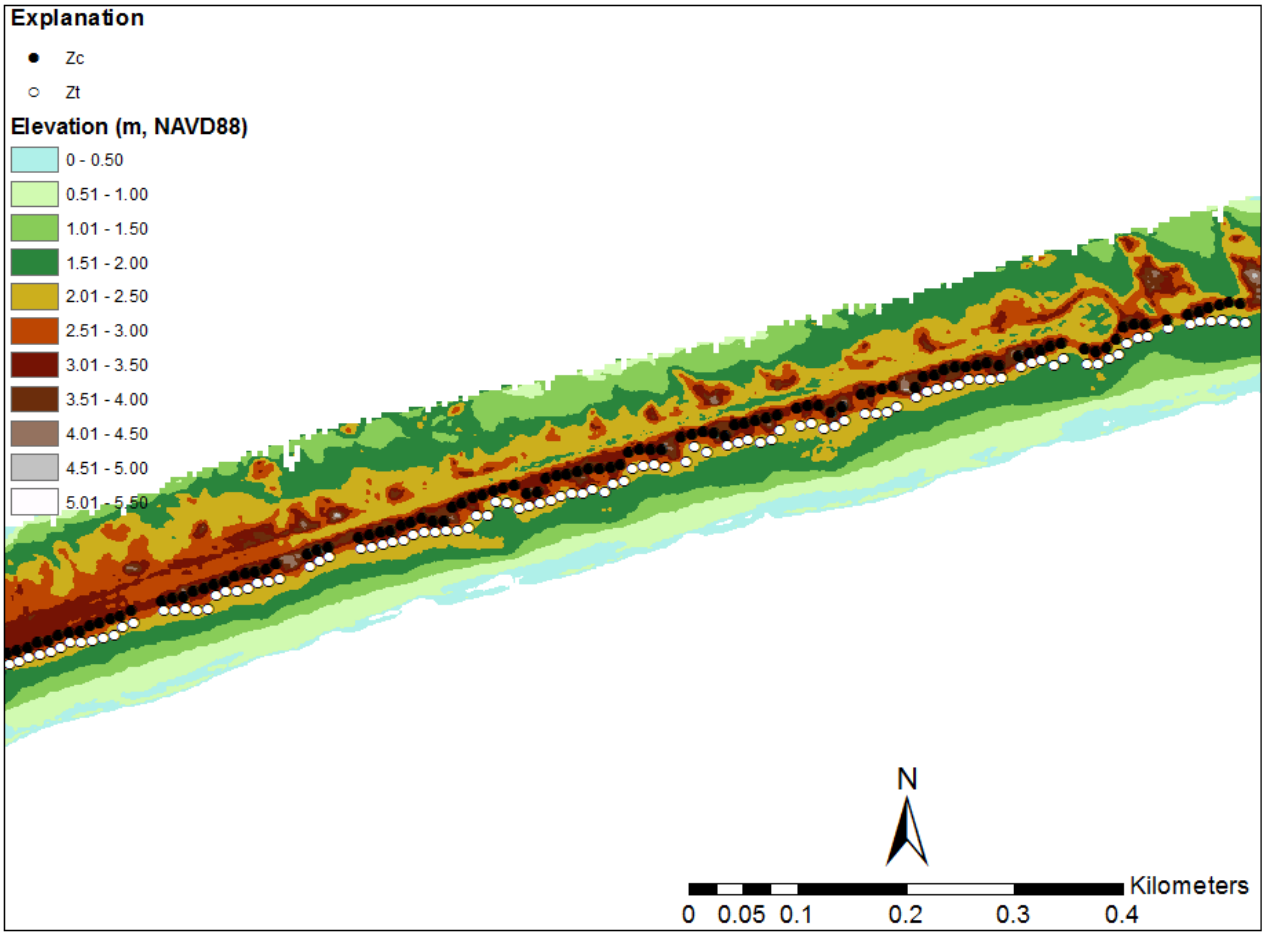

Figure 8. Automatically extracted dune crest (z_c) and toe (z_t) overlain on three-dimensional gridded lidar topography from Santa Rosa Island, Florida, collected September 8, 2008, after the landfall of Hurricane Gustav. Gaps in the data indicate locations where the automated algorithm was unable to identify a dune crest. Abbreviation: m, meter.

2.1.3 Dune Toe

Specification of the elevation and cross-shore location of the dune toe (x_t,z_t) is essential both for differentiating between swash and collision storm regimes and for computing beach slope. A hydrodynamic-based elevation criteria, the high water line (HWL), was used to distinguish between swash-generated berms and aeolian-generated dunes in order to avoid selection of a dune toe on a berm (fig. 7). The HWL, which has contributions from both waves and tides, was defined as the sum of MHW elevation and a 20-year (yr) 2-percent exceedance runup level (Ruggiero and List, 2009). The

runup elevation was parameterized using Stockdon and others (2006) and a 20-yr mean wave height (H_s) and peak period (T_p) from the U.S. Army Corps of Engineers Wave Information System (WIS) hindcasts (μH_s = 0.85 m, σH_s = 0.22 m; μT_p = 5.90 seconds (s), σT_p = 0.34 s). The resulting HWL elevation around the Gulf of Mexico basin was approximately 60 cm NAVD88. Local HWL values were calculated as the spatial mean within a 2-km sliding window. An error of 40 cm was included to account for uncertainty in wave runup computations (Stockdon and others, 2006), lidar data uncertainty, and spatial variability with the 2-km window. If the dune crest elevation (z_c) did not exceed the elevation of HWL, then the feature was classified as a berm peak and x_t and z_t were not determined.

Where z_c was greater than HWL, the feature was assumed to be a dune, and x_t and z_t were mathematically derived from beach profiles using a process similar to the automated method of dune crest identification. Dune toe was defined as the location of maximum slope change between x_c and x_{sl}. The cross-shore location of the dune toe was constrained in the landward limit by the primary dune crest location and at the seaward boundary by the shoreline location. Additionally, the dune toe was restricted to locations where:

- z_t > HWL to ensure that a water-laid feature was not selected,
- $z_c - z_t > 0.5$ m to prevent selection of small depressions on the dune face itself, and
- curvature of the profile around the (x_t,z_t) was negative.

Similar to the dune crest analysis, (x_t,z_t) identified by the automated process was checked by viewing ArcGIS shapefiles of the dune toe in overlay with the dune crest and gridded lidar datasets (fig. 8). The shape of a natural beach can vary greatly from the idealized dune profile, and visual verification ensured spatially consistent dune features are chosen.

2.1.4 Beach slope

Wave runup is dependent on the local beach slope over which the swash progresses as it interacts with the beach or dune. Under average wave conditions, swash flows up- and down-slope within a short horizontal distance (meters) of the MHW shoreline, an area defined as the foreshore. However, during a hurricane, storm surge can raise the still water level to meters above the MHW shoreline. Therefore, the landward limit of storm-induced swash excursion is constrained by the base of the dune (x_t,z_t). If a dune is not present, then the berm crest (x_c,z_c) becomes the landward swash limit. Using these features as landward limits and the shoreline (x_{sl}) as the seaward, the mean beach slope (β_m) was calculated using an endpoint method (fig. 7).

2.2 Hurricane-induced water levels

During a hurricane, water levels at the shoreline include the combined effects of tide, storm surge, and local wave-driven swash and setup, the super-elevation of the water surface at the shoreline due to wave breaking. Predictions of coastal change during hurricanes require estimates of both the mean water level and the wave runup that can be expected for each category. The mean hurricane-induced water level, η_{50} , is defined as

$$\eta_{50} = \eta_{tide} + \eta_{surge} + \eta_{setup} \quad (1)$$

where η_{tide} is the astronomical tide level, η_{surge} is storm surge, and η_{setup} is wave setup. The extreme water levels attained during the storm include wave swash, the time-varying component of wave energy on the beach, and are defined as

$$\eta_{98} = \eta_{50} + 1.1(S/2) \quad (2)$$

where S is the total swash excursion about the setup level and the 1.1 multiplier corrects for parameterization bias. It is important to note that both the mean and maximum water levels include a

contribution from waves, which can increase water levels at the shoreline by the same magnitude as surge for category 1- 3 hurricanes (Stockdon and others, 2007a).

2.2.1 Tide and Storm Surge

The predicted elevations of combined high tide and storm surge ($\eta_{tide} + \eta_{surge}$) for category 1-5 hurricanes were extracted from the National Oceanic and Atmospheric Administration (NOAA) SLOSH (Sea, Lake, and Overland Surges from Hurricanes) model, which has been employed by NOAA in inundation risk studies and operational storm surge forecasting. The numerical model is based on linearized, depth-integrated equations of motion and continuity (Jarvinen and Lawrence, 1985). Storm surge is modeled by simulating the conditions of each category storm approaching the coast from different angles and at varying speeds. Changes in maximum surge elevations are forced by time-varying wind-stress and pressure-gradients that depend on the hurricane location, minimum pressure, and the radius of maximum winds (Jarvinen and Lawrence, 1985).

Storm surge levels ($\eta_{tide} + \eta_{surge}$) are simulated for each storm category in each of 16 model domains subdividing the gulf coast region. These simulations represent the peak water levels in each domain forced by thousands of hypothetical storms of varying forward speed, size, and direction, under mean higher high water tide conditions. The maximum surge within each grid cell, or the Maximum of the Maximum (MOM), represents a worst-case, localized surge level that could occur for a nearby hurricane landfall (fig. 9). (Note that the MOM is a composite from many storms and does not represent water levels that would occur along the entire coast for a single storm.) The resulting spatial variations in maximum storm surge reflect local water depths, proximity to bays and rivers, and so on and are accurate to ±20 percent of the calculated value (NOAA, 2007). Prediction errors in the SLOSH model can arise from differences between the parametric wind models, which force SLOSH, and the actual

hurricane wind field (Houston and others, 1999) as well as discrepancies between the coarse model grid and the real topography and bathymetry over which the storm will travel.

Several additional constraints were applied to address some practical implementation problems associated with our use of the MOMs. First, SLOSH model domains were constructed to focus highest grid resolution in the most vulnerable coastal regions (fig. 9). As a result, the different model domains overlap with each other. In these cases, MOM results were weighted to give preference to (1) results produced nearer the focal region of one of the overlapping grids, (2) results from higher resolution grid cells, and (3) more recently published results. Preference was given to different grid cells by scaling their results by a factor of 1 for the smallest cells to zero for the largest cells. Resulting surge levels were interpolated, incorporating the assigned scaling factor, to the evenly spaced shoreline and smoothed with a Hanning window set to a length of 2 km alongshore. Additionally, since topographic and hydrodynamic results are compared to each other, we converted all elevations to the same NAVD88 vertical datum (using the same GEOID model).

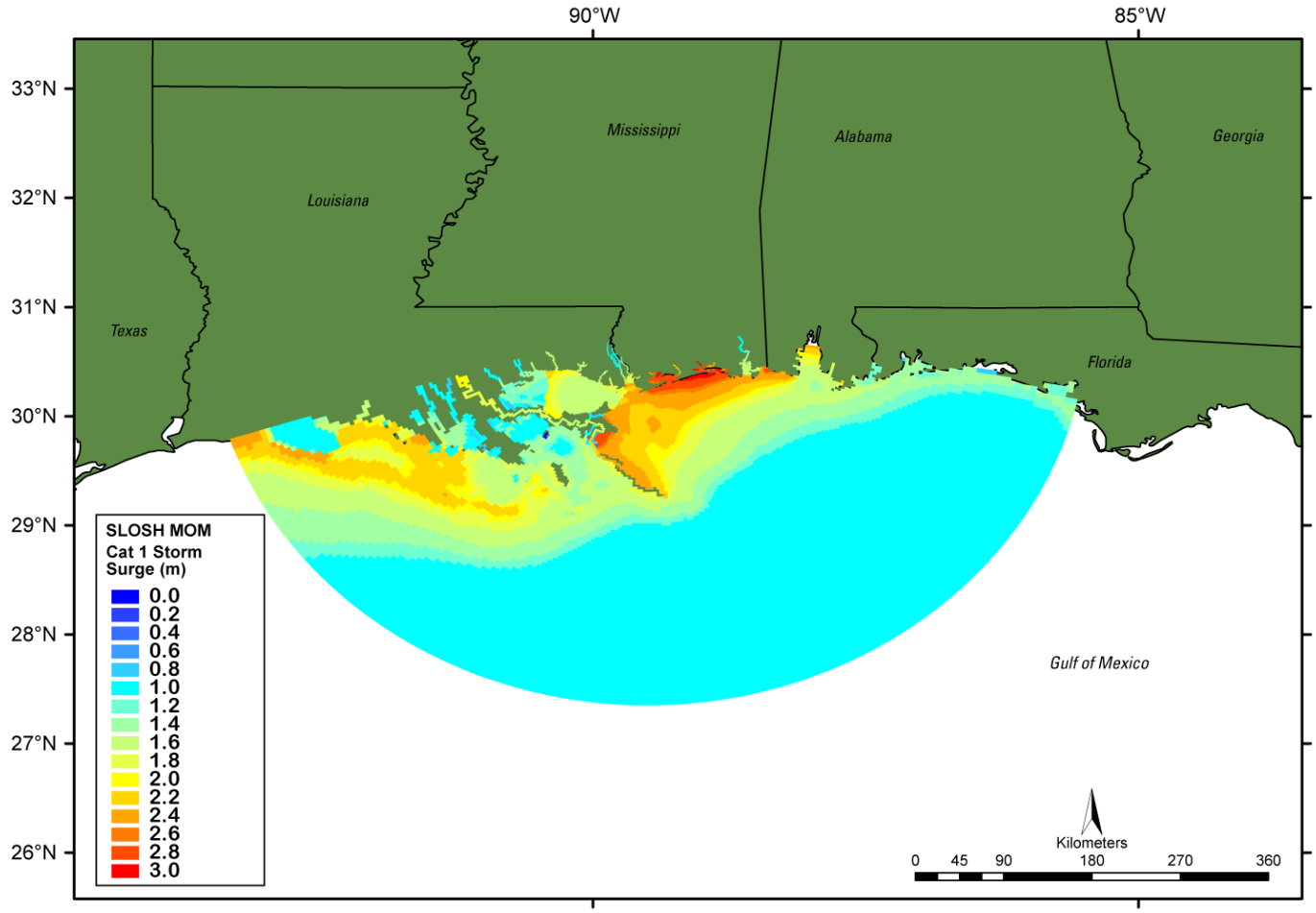

Figure 9. Sea, Lake, and Overland Surges from Hurricanes (SLOSH) category 1 modeled surge Maximum of the Maximum (MOM) for the New Orleans basin. Abbreviation: m, meter.

2.2.2. Wave Height and Period

Wave conditions vary spatially and temporally during hurricanes due to the same factors that cause variation in storm surge. Unfortunately, there is no equivalent of the MOMs that can be used to specify maximum wave height and period for category 1-5 hurricanes. Observations during hurricanes are incomplete as buoys tend to fail during conditions stronger than tropical storm. Long-term hindcasts of historical wave conditions (for example, USACE WIS) also under-represent storm conditions. Therefore, wave conditions were estimated using Simulating WAves Nearshore (SWAN) model, a

spectral wave model that resolves random, short-crested wind-generated waves varying in time and space (Holthuijsen and others, 1993).

One approach to calculating storm-wave parameters would be to simulate individual idealized hurricanes in SWAN, much like was done with SLOSH in order to build a MOM-consistent dataset. However, an attempt to cover the entire Gulf of Mexico coastline with idealized hurricane tracks, and include a sufficient sampling of storm parameter space (wind speed, radius of maximum winds, forward speed, and so on), would require a massive computational effort. Furthermore, because we require wave information at a specific shallow water depth (20 m), the height of hurricane waves will tend to be limited by dissipation due to breaking, white-capping, and friction. Consequently, the sensitivity of parameterized shoreline water levels to wave parameter errors is expected to be limited as well.

Therefore, we apply a simple approach of generating stationary waves (in time) using SWAN for the maximum wind speed that defines each hurricane category over the entire Gulf of Mexico. For determination of the contribution of waves to the total hurricane-induced water levels, the maximum wave-height value from an ensemble of simulations of the maximum wind speed was selected as the representative value for each category, very similar to the MOM product from the SLOSH model. As with the MOMs, these results do not represent an individual storm but rather a composite of many storms.

For our analysis, SWAN version 40.85 was used. The model was run in third-generation mode using the Westhuysen formulation for white-capping and Yan formulation for wind input (GEN3 WESTH). Bottom friction was included using default values, and all other model parameters were left as default. The longitudinal resolution of the SWAN computational grid was 3.34 km. The latitudinal resolution varies from 2.87 km in the northern gulf to 3.17 km at the southern limits (fig. 10). SWAN was run 24 times for each wind speed with direction varying from 15° to 360° by 15° (fig. 10). For each

wind speed the model results from the 24 wind direction runs were combined by retaining the wave parameters from the wind direction that generated the largest significant wave height (H_s) in each grid cell.

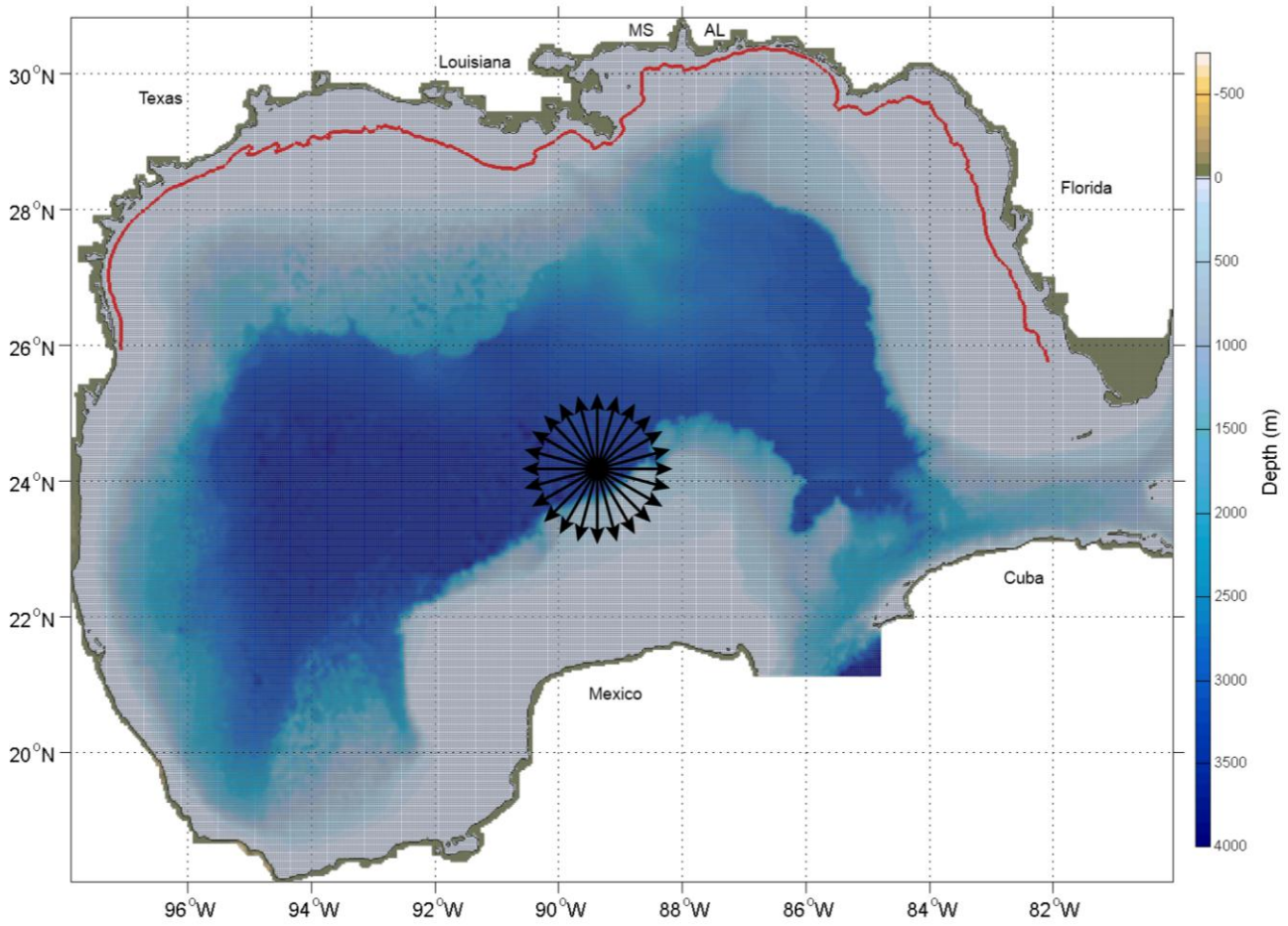

Figure 10. Simulating WAves Nearshore (SWAN) computational grid containing 169,188 active nodes. Longitudinal resolution is 3.34 kilometers and latitudinal resolution varies from 2.87 kilometers in the northern Gulf of Mexico to 3.17 kilometers in the south. The 20-meter isobath along the U.S. coastline is shown in red. Arrows indicate 24 wind directions used in simulation. Abbreviation: m, meter.

Simulated H_s at the 20-m isobaths for category 1-5 hurricanes was relatively uniform around the Gulf of Mexico basin (fig. 11). The resulting maximum wave heights at the 20-m isobaths typically ranged from about 7 m to about 9 m, except where the continental shelf was very narrow. To put these model results in context, we compared the modeled wave heights to observed wave heights at several

buoys located in different water depths throughout the Gulf of Mexico. Maximum observed wave heights were between 6 m and 9 m at relatively shallow locations (that is, 15 to 30 m water depths, which included just three buoys). The simulated wave heights are representative of maximum possible wave heights for each hurricane category.

Mean period estimates ranged between 7 and 18 s and tended to be higher where the significant wave height was higher (again, due to the presence or absence of dissipation). The swash parameterization requires estimates of peak period, which were not reliably estimated due to our simplified wind field. Consistent peak-period estimates were obtained from an analysis of 20 years of NOAA National Data Buoy Center data for 15 shallow-water buoys operating in the gulf. The analysis yielded a parameterized relationship between significant wave height, obtained from the SWAN model, and peak wave periods (fig. 12).

$$T_p = b_0 + b_1 * H_s + b_2 * H_s^2 + b_3 h, \quad (4)$$

where Tp is peak wave period, H_s is significant wave height, and h is the depth corresponding to each wave period and height. Data from all buoys in water depths less than 30 m were used in a linear regression to estimate the model coefficients, b_n, resulting in

$$b_0 = 3.8460\ (\pm 0.0617)$$

$$b_1 = 1.7812\ (\pm 0.0289)$$

$$b_2 = -0.0120\ (\pm 0.0052)$$

$$b_3 = -0.0049\ (\pm 0.0957)$$

This parameterization was used to compute wave periods for each hurricane category that were consistent with Gulf of Mexico observations, using the simulated significant wave heights and the 20-m depth as input. Recomputed wave periods typically increase from about 16 s to 22 s (fig. 11).

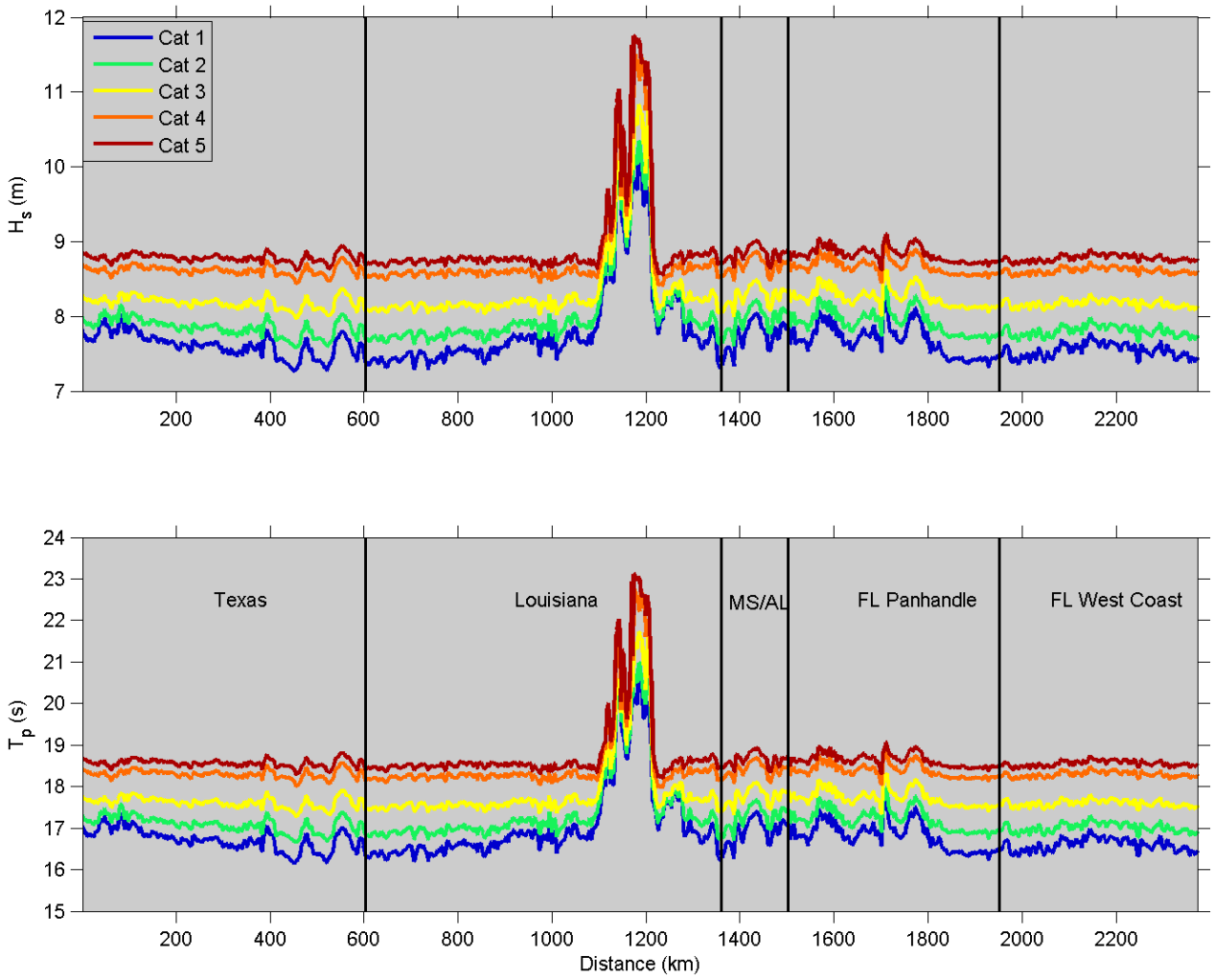

Figure 11. Modeled significant wave height (H_s, top) and parameterized peak period (T_p, bottom) at the 20-meter isobath around the Gulf of Mexico extending from Texas (left) to the Florida west coast (right). State boundaries are indicated by vertical lines. Abbreviations: m, meter; km, kilometer; s, second.

Figure 12. Significant wave height (H_s) and peak (T_p) wave periods for deep (water depth, h, > 30 m; black) and shallow (h < 30 m; red) water observed at National Data Buoy Center (NDBC) buoys in the Gulf of Mexico. The weighted regression based on shallow water buoys is shown in red. Abbreviations: m, meter; s, second.

2.2.3 Wave Setup and Swash

Swash and setup, the wave-induced components of total water level at the shoreline, are parameterized using modeled wave conditions and measured beach slope (Stockdon and others, 2006). Setup is parameterized as

$$\eta_{setup} = 0.35\beta_m(H_0L_0)^{1/2} \quad (5)$$

where $L_0 = gT_p^2/2\pi$. Wave swash, *S*, the time-varying component of water levels at the shoreline, is parameterized as

$$S = \left[H_0 L_0 (0.563\beta_m{}^2 + 0.005)\right]^{1/2} \quad (6)$$

Combining equations (5) and (6) with modeled estimates of $\eta_{tide} + \eta_{surge}$ provided estimates of hurricane-induced mean and maximum water levels (equations 1 and 2).

2.3 Probability of coastal change

Probabilities of coastal change are based on estimating the likelihood that the beach system will experience erosion and deposition patterns consistent with collision, overwash, or inundation regimes. Uncertainties that were considered arise from topographic elevation errors (for example, lidar error and interpolation error) and errors associated with predicting wave runup elevations.

The probabilities of collision (dune erosion), overwash, and inundation were calculated using distributions of morphologic and hydrodynamic parameters extracted from 1-km sections of coast. Hydrodynamic and morphologic data were co-located alongshore using a common reference line (the 20-yr HWL shoreline). Morphologic features, z_c, z_t, and β_m, were interpolated to the reference line and smoothed using a Hanning window with a full width of 2 km. Each interpolated, smoothed value of (x_c,z_c), (x_t,z_t), and β_m was assigned a RMS error calculated from the scatter of the data in the smoothing window (fig. 13, top). The variables were represented with a normal distribution of values at each location, now with a 1-km alongshore spacing, using the interpolated value as the mean and the RMS error as the standard deviation *(*fig. 13, bottom). This produced mean and standard deviations for both the hydrodynamic and the morphologic variables.

Using the statistical distribution of the input values at each alongshore location, the probability, *p*, that the total water level exceeds the dune crest or toe elevation threshold for a particular storm regime is calculated from the normal cumulative distribution function

$$p = \frac{1}{\sigma\sqrt{2\pi}} \int_0^{\infty} e^{\frac{-(t-\mu)^2}{2\sigma^2}} dt \qquad (7)$$

where μ is the mean difference between the either the mean (inundation) or extreme (collision, overwash) water levels and either the dune toe (collision) or dune crest (overwash, inundation) regime. The variance of the difference, σ^2, is the sum of the variances of the inputs. Thus, the probabilities of each storm-impact regime are calculated as:

- collision: $p_c = probability([\eta_{98} - z_t] > 0)$
- overwash: $p_o = probability([\eta_{98} - z_c] > 0)$
- inundation: $p_i = probability([\eta_{50} - z_c] > 0)$

For example, figure 13 shows the cumulative distribution of $(\eta_{98} - x_c)$ for a 1-km section of coast for a category 1 hurricane. The probability that this value exceeds zero defines the likelihood that overwash will occur at this location.

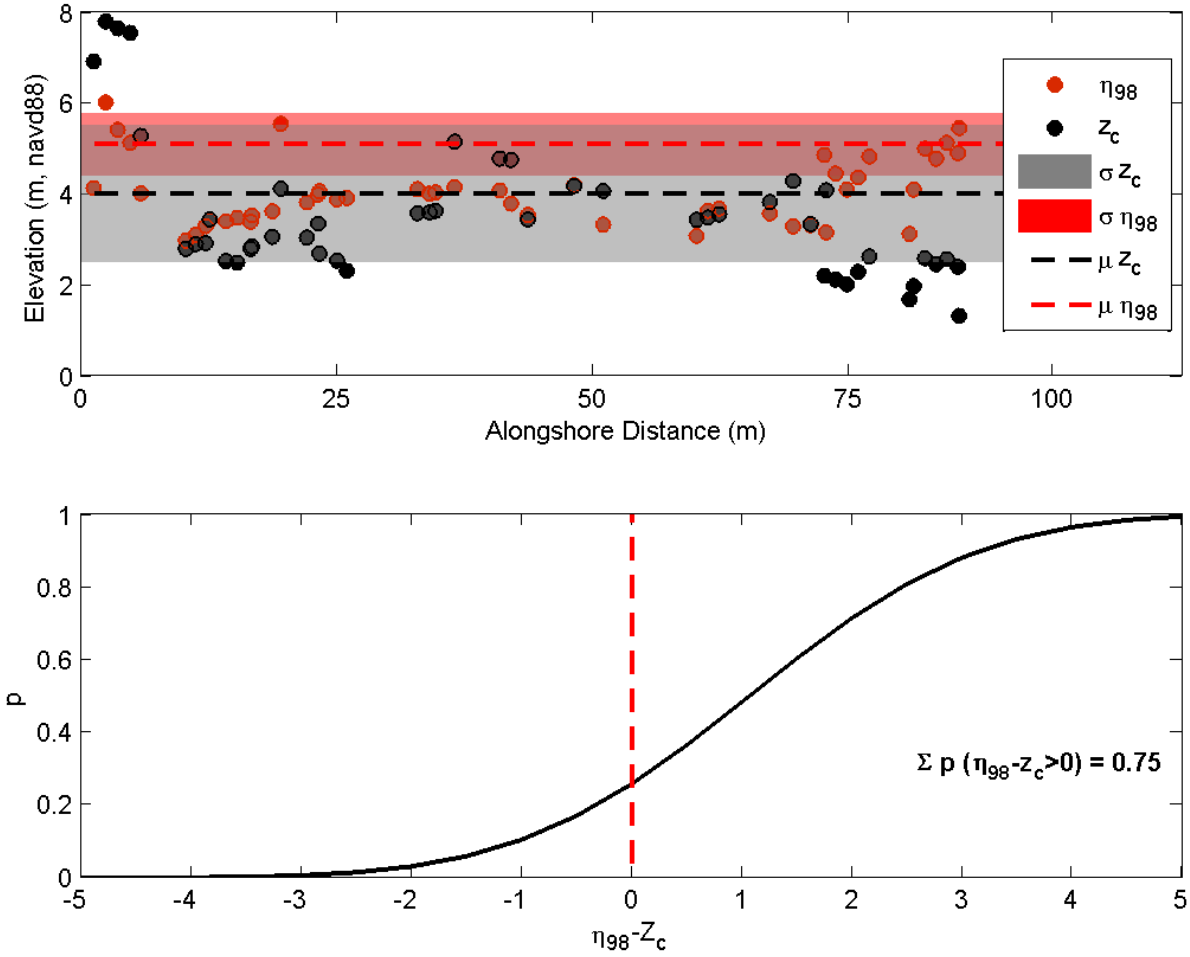

Figure 13. Maximum shoreline water level (η_{98}) for a category 1 hurricane and raw and smoothed dune crest elevation (z_c) for a 1-kilometer alongshore section (top). Shaded areas indicate the RMS error about the mean value within the section. Cumulative probability distribution, $p(\eta_{98}\text{-}z_c)$ where the sum of p over the range $(\eta_{98}\text{-}z_c)>0$ defines the probability of overwash (bottom). Abbreviation: m, meter.

3. Results

3.1 Coastal morphology

Dune morphologies around the Gulf of Mexico vary extensively over both short and long spatial scales (ta1ble 1). Mean dune crest elevation, μz_c, for sandy beaches along the gulf coast is 2.42 m, and the standard deviation, σ, is 1.02 m, indicating spatial variability high enough that low elevations (μ –

2σ) are just above the HWL (fig. 14a). Elevations range from 0.5 to over 8 m. Dune toe elevations are consistently low with less spatial variability (fig. 14b; μz_t = 1.60 m; σz_c = 0.59 m). In general, local spatial variability scales with dune elevation: locations with higher mean elevations also exhibit greater spatial variability (fig. 15).

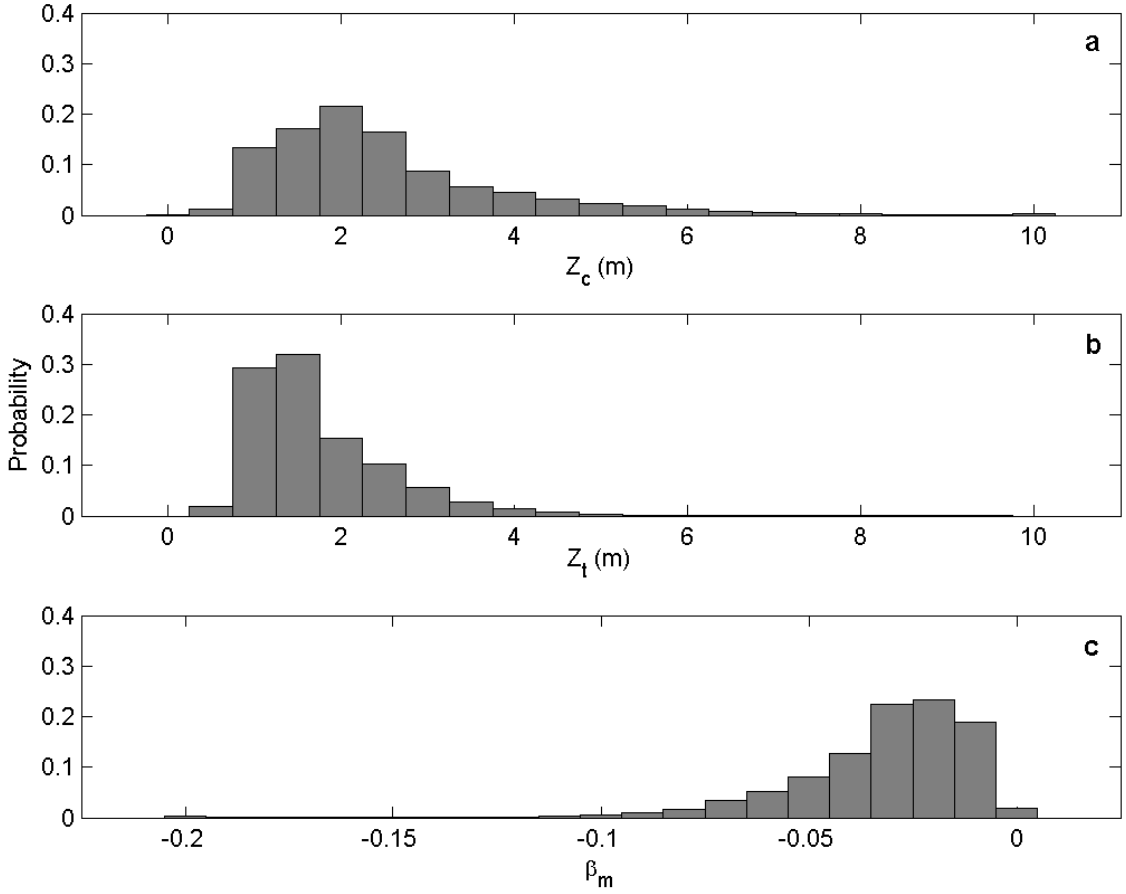

Figure 14. Distributions of dune crest elevation (z_c, a), dune toe elevation (z_t, b), and mean beach slope (β_m, c) for the U.S. Gulf of Mexico sandy coastlines. Abbreviation: m, meter.

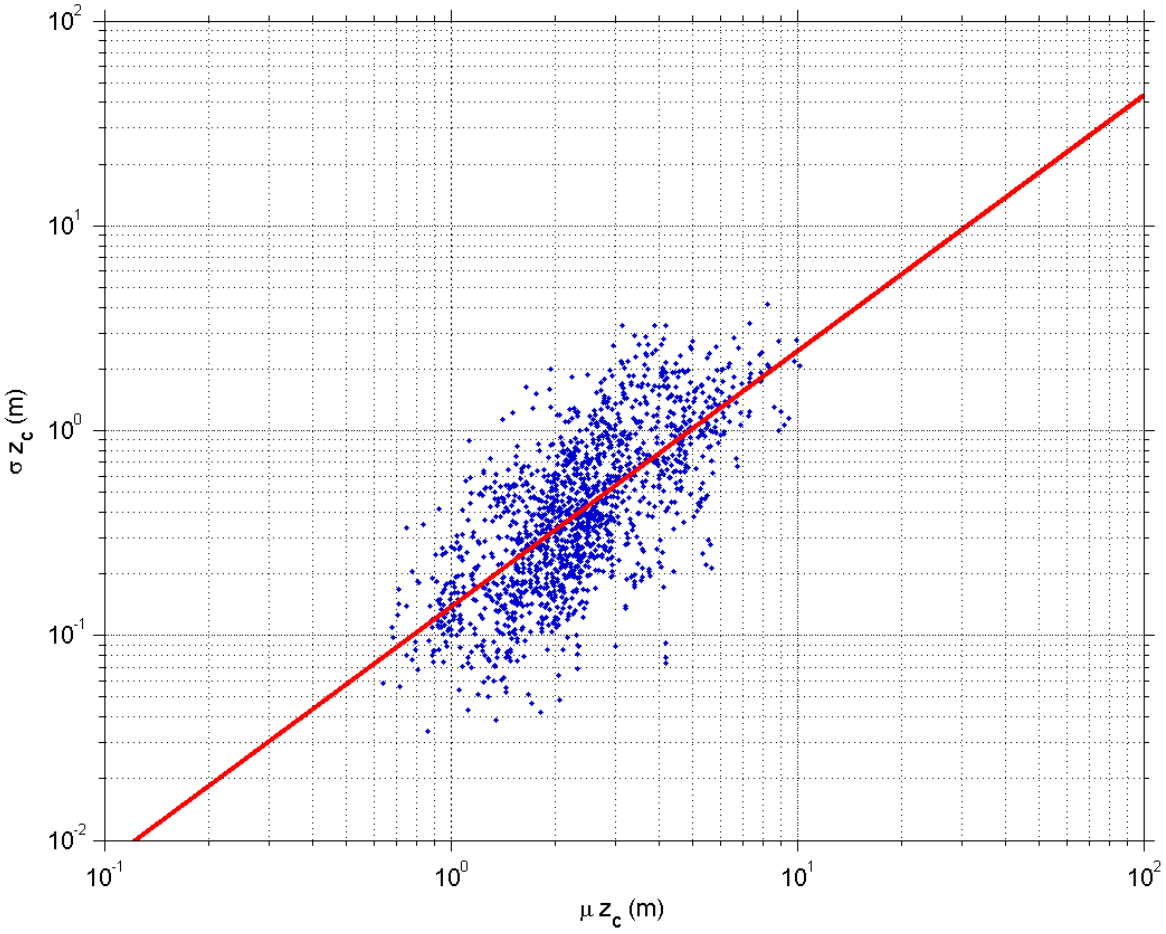

Figure 15. Mean dune crest elevation (μz_c) for 1-kilometer sections of coastline compared to the standard deviation (σz_c) in those section. r^2 = 0.48, N = 1620. Abbreviation: m, meter.

The highest dunes (z_c in excess of 8 m) are located in south Texas and in the Florida Panhandle (figs. 16-17); however, variability is high in both States, as noted by σz_c of 1.50 m (μz_c = 2.72 m) and 1.69 m (μz_c = 3.18 m), respectively. Some of the lowest elevations are also found in Florida, located along the west-central coast (μz_c = 1.84 m, σz_c = 0.74 m). However, the lowest dunes are found in Louisiana (μz_c = 1.57 m, σz_c = 0.64 m), particularly along the bermed beaches of the Chenier plain, where beach ridges and berms mix with muddy coasts and marshes (fig. 17; distance, y, = 700-775 km). Louisiana beaches also have the lowest dune toes (figs. 16-17).

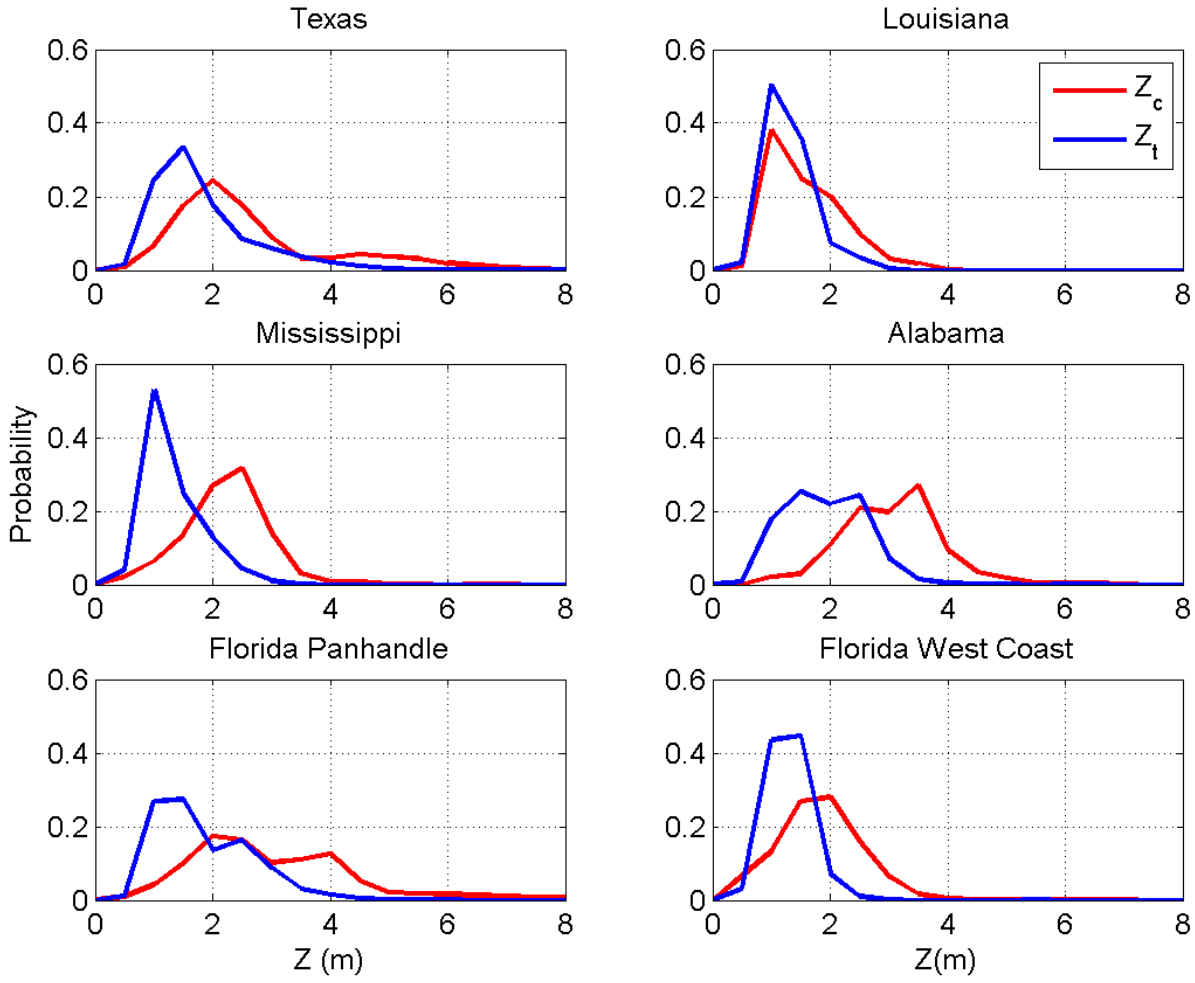

Figure 16. Distribution of dune crest (z_c) and dune toe (z_t) elevations for Texas, Louisiana, Mississippi, Alabama, Florida Panhandle, and Florida west coast. Abbreviation: m, meter.

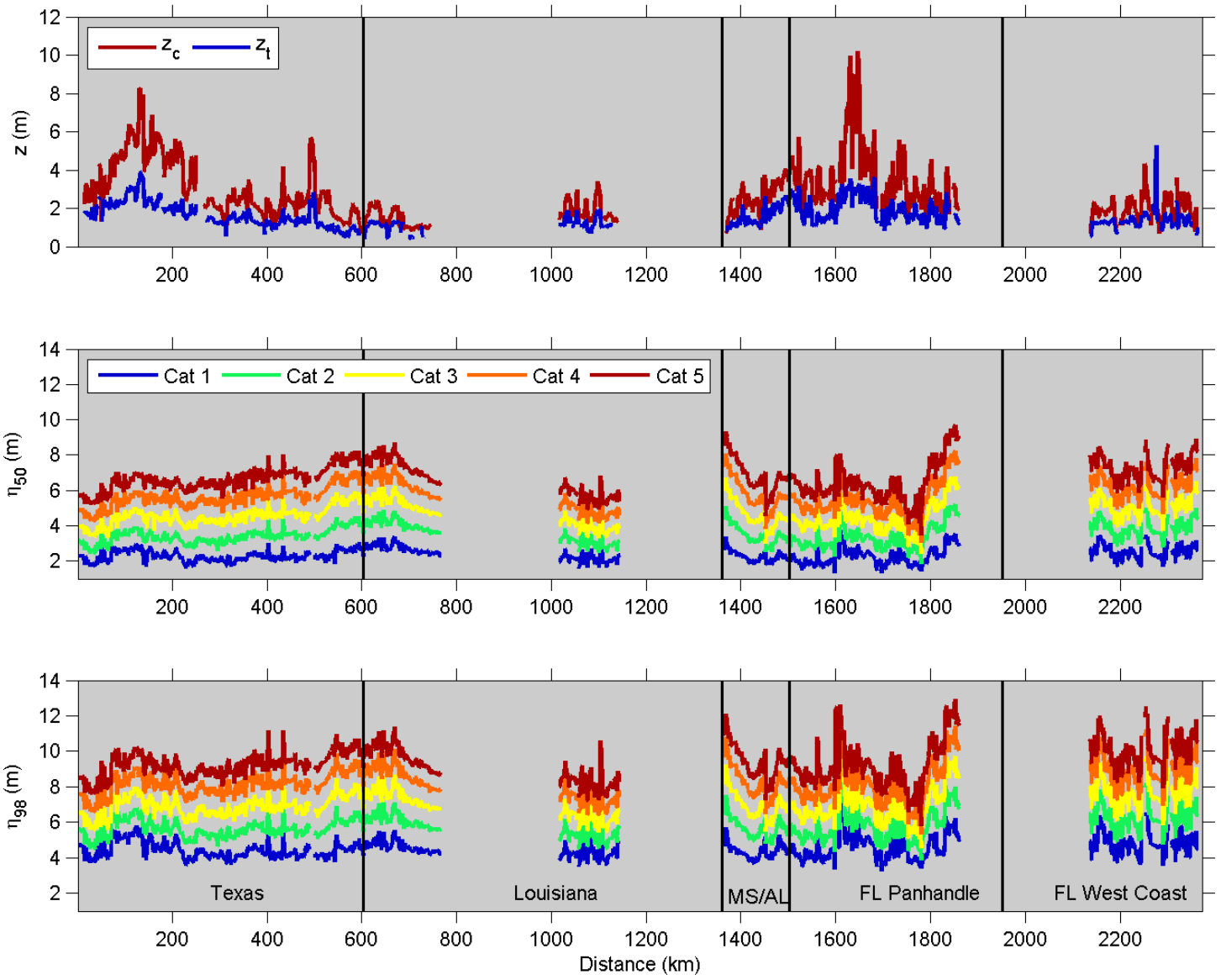

Figure 17. Dune crest (z_c) and toe (z_t) elevations (top) and hurricane-induced mean (η_{50}; middle) and maximum (η_{98}; bottom) shoreline water levels around the Gulf of Mexico extending from Texas (left) to the Florida west coast (right). State boundaries are indicated by vertical lines. Gaps in the data are locations of marshy shorelines. Abbreviation: m, meter; km, kilometer.

While also spatially variable, mean beach slope is generally low (fig. 18), leading to dissipative conditions during storms. The lowest slopes, and least spatial variability, are located along the Mississippi coast ($\mu\beta = 0.016$, $\sigma\beta = 0.009$). Steeper slopes are present along the central Florida west coast ($\mu\beta = 0.047$); however, the standard deviation was also greatest here ($\sigma\beta = 0.033$).

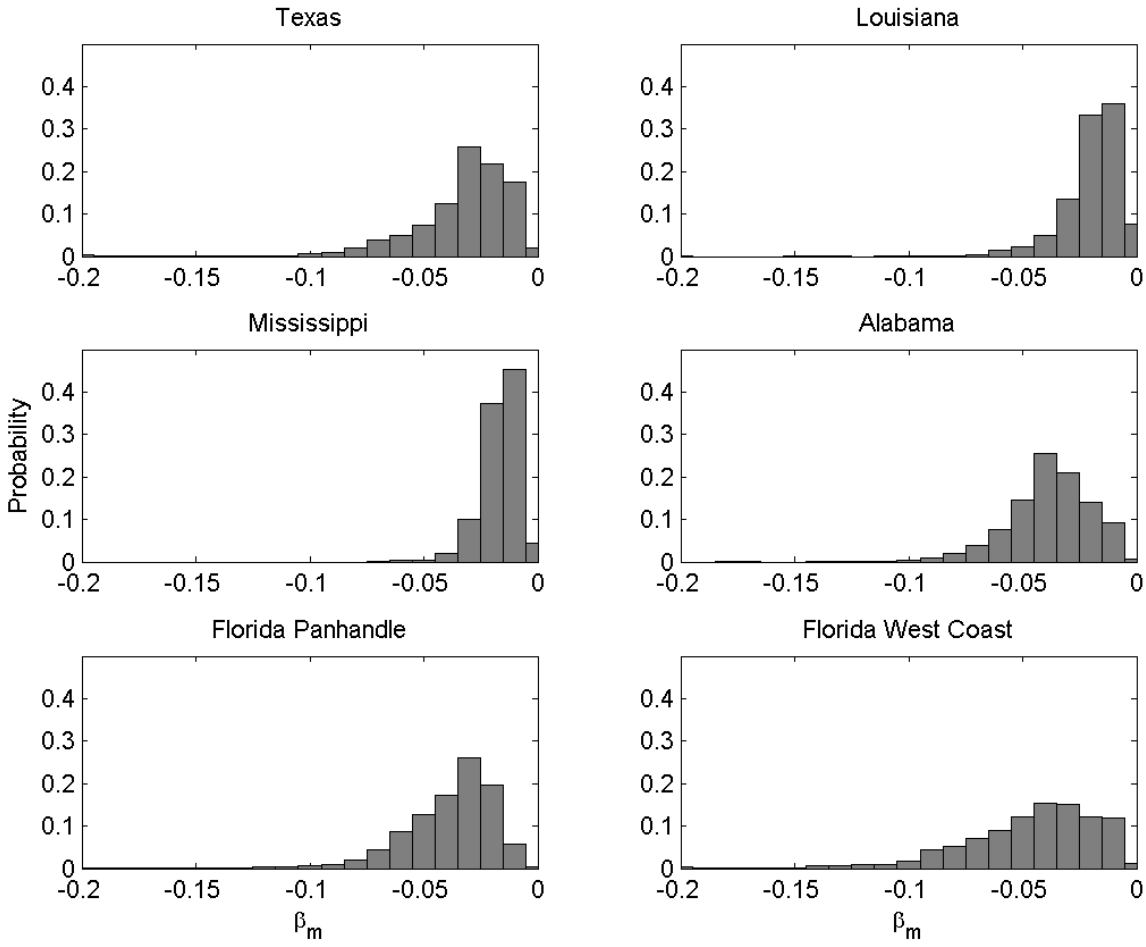

Figure 18. Distributions of mean beach slope (β_m) elevations for Texas, Louisiana, Mississippi, Alabama, Florida Panhandle, and Florida west coast.

3.2 Hurricane-induced water levels

The variability of hurricane-induced water levels can be attributed to both hydrodynamics and beach morphology. Variability of H_s at h = 20 m within a single category, due to local bathymetry and dissipation from depth-limited breaking, white-capping, and bottom friction, leads to corresponding alongshore differences in η_{98} and η_{50}. The largest waves (H_s = 10-13m) were located offshore of the Mississippi River Delta where a narrow shelf allows larger waves to make it to the nearshore (fig. 11), as wave breaking and, to a lesser extent, bottom dissipation act over very short distances before reaching the 20-m isobath. However, for the sandy beaches used in this analysis, variability of H_s along the shoreline for a single category is minimal; standard deviation of H_s ranges from 14 cm for a category 1 storm to 6 cm for a category 5 storm (table 2).

Smaller scale spatial variability of η_{98} (fig. 18) is dominated by alongshore variations in β_m, as the wave-driven components of shoreline water levels, η_{setup} and S, are dependent on both input wave conditions and local slopes (equations 5 and 6). For similar input wave conditions, steeper beach slopes result in higher total runup elevations (η_{R2} = 1.1(η_{setup} + $S/2$)). For example, modeled category 3 wave heights were 8.2 m for both the Mississippi and west-central Florida coastlines. However, η_{R2} is a meter higher on the Florida west coast than in Mississippi because of the steeper slopes: β_m = 0.047 in Florida as opposed to β_m = 0.016 in Mississippi.

The modeling exercise demonstrated the relative importance of waves with respect to storm surge. For a category 1 storm, wave-driven components represent 63 percent of the total hurricane-induced water levels: the remaining 27 percent is attributed to tides and surge (table 2). For a category 2 storm, the contributions are approximately equal, 51 percent from waves and 51 percent from combined tides and surge. In a category 5 hurricane, surge dominates the signal, contributing 64 percent to the total

water-level elevation. Wave height does not grow as rapidly due to dissipation through white-capping and breaking; however, surge continues to grow, approximately 1 m with each category.

3.3 Probability of Coastal Change

The probabilities of collision, overwash, and inundation indicate whether a specified coastal change regime is very likely (probability >90 percent), likely (>66 percent), about as likely as not (33 to 66 percent), unlikely (<33 percent), and very unlikely (<10 percent) given the local landfall of each hypothetical storm scenario. (Range descriptions are based on guidance from the Intergovernmental Panel on Climate Change (IPCC) (Le Treut and others, 2007).) Probabilities of coastal change for the lowest category hurricane show the extreme vulnerability of beaches throughout the Gulf of Mexico to dune erosion and overwash (figs. 19-20). For direct landfall of the lowest category hurricane, 99 percent of sandy beaches are very likely to experience dune erosion due to collision and over 70 percent of the coastal areas are vulnerable to overwash (table 3). Inundation of the beach and dune system is expected along 27 percent of the coastline, typically near inlets (for example, the Mississippi barrier islands; fig. 21) and in areas with low elevation beach berms (the Chenier plain of Louisiana, fig. 20, and west-central Florida where μz_c < 2 m; table 1). For a category 3 hurricane landfall, 92 percent of the beaches in the Gulf are very likely to experience overwash and associated beach and dune erosion (table 3), and the percentage of beaches that are very likely to be inundated climbs to 73 percent. The basin-wide average storm surge associated with category 3 wind speeds exceeds 4 m, over 1.5 m higher than the average dune and berm elevation, μz_c = 2.43 m.

The higher dune elevations in the Florida Panhandle are less vulnerable to coastal change. During a category 1 landfall, 98 percent of these beaches are likely to experience dune erosion; however, only 47 percent are expected to overwash (fig. 20). On the west-central Florida coast, vulnerability to dune

erosion during a category 1 hurricane is the same, 99 percent, but crest elevations are more than 1 m lower than those on the panhandle, leading to increased vulnerability to overwash–98 percent of sandy beaches (fig. 20; table 3). For conditions related to a category 3 hurricane, 99 percent of Florida west coast beaches are very likely to inundate compared to only 51 percent of panhandle beaches.

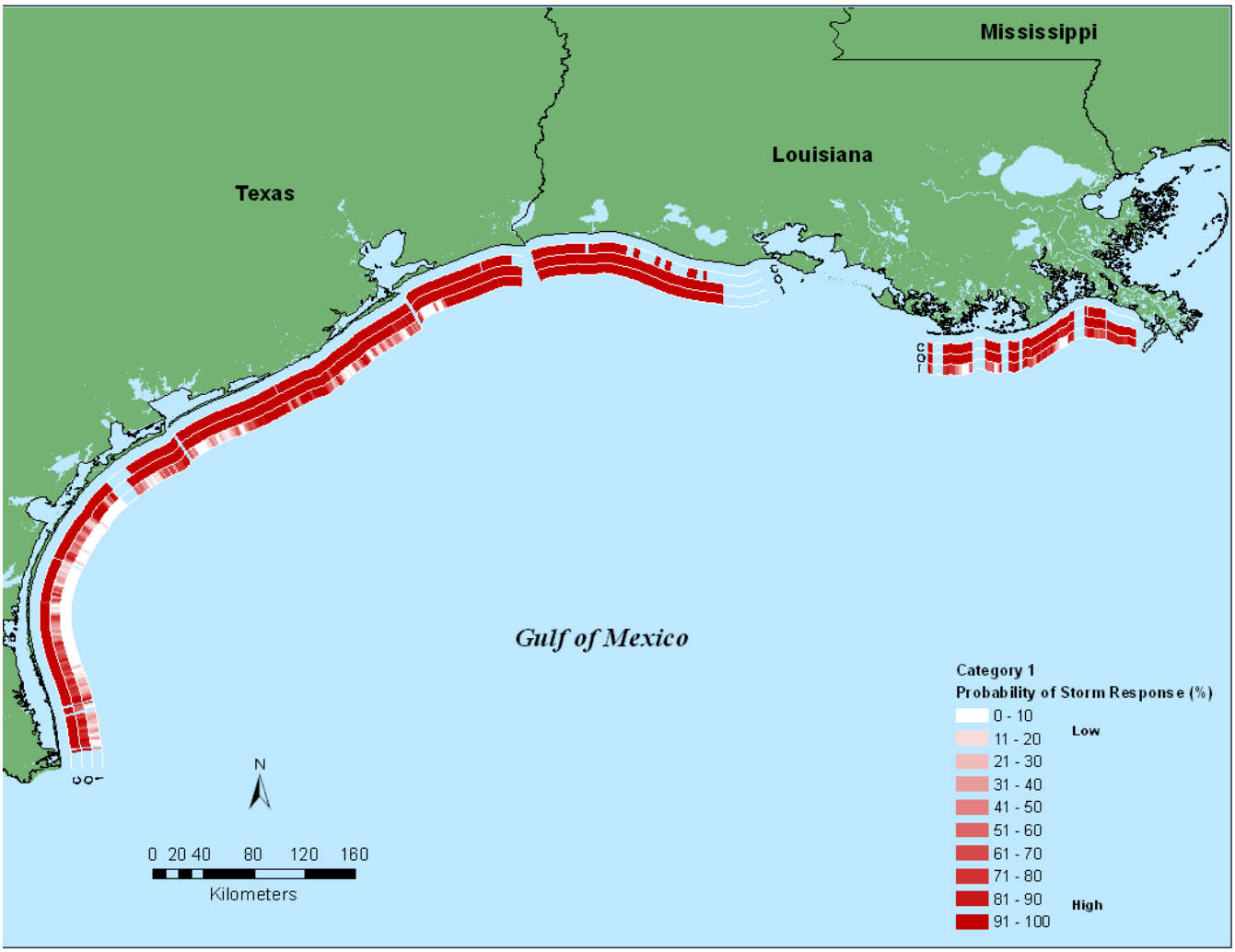

Figure 19. Probabilities of collision (c), overwash (o), and inundation (i) during a category 1 hurricane for Texas and Louisiana.

Spatial variability exists over smaller spatial scales on the order of kilometers in areas with complex dune fields or more three-dimensional beach morphology. For example, in south Texas, the mix

of low and high dunes leads to a more complicated picture of hurricane-induced erosion hazards (fig. 19). The smaller scale variability (alongshore spacing of 1 km) for a specific area can be examined using interactive maps that are available online. The probability of each mode of coastal change for category 1-5 landfalls, as well as supporting morphology and water level data, are available online (*http://coastal.er.usgs.gov/hurricanes/erosionhazards/gom/*).

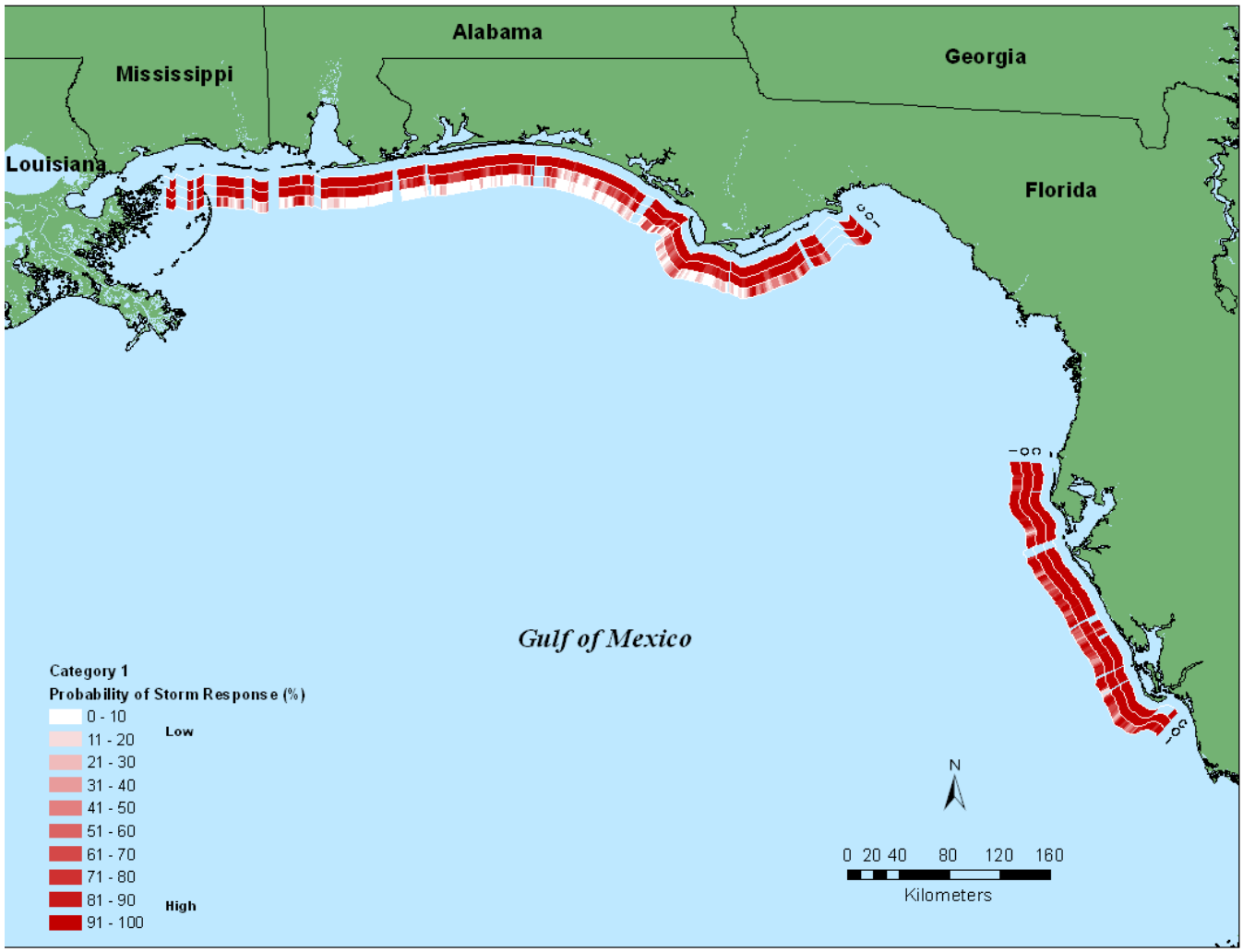

Figure 20. Probabilities of collision (c), overwash (o), and inundation (i) during a category 1 hurricane for Mississippi, Alabama, and west Florida.

4. Discussion

4.1 Validity of assumptions

This analysis is based on an estimate of a worst-case scenario with respect to storm surge levels and wave heights associated with each hurricane category. The implied assumption is that each location along the coast experiences the right-front quadrant of the hurricane at landfall. This results in onshore-directed winds and the combined effects of both the circulation and the forward motion of the storm.

Waves and surge associated with an actual storm may be significantly different than model results. The SLOSH results are grouped by Saffir-Simpson categories, which are based on wind speeds. It is recognized that wind-based Saffir-Simpson categories are not always an accurate indicator of expected storm surge (Irish and others, 2008; Irish and others, 2009); however, they do provide a convenient way to represent the data based on storm intensity, allowing users to examine a range of conditions in a small number of scenarios. Real-time analysis of individual landfalling hurricanes includes more realistic updates of surge, tides, and waves (*http://coastal.er.usgs.gov/hurricanes/*).

This assessment also assumes that the existing lidar-surveyed topography is up to date and accurately and synchronously reflects dune and beach morphology. Significant changes to beach and dune morphology between the survey date and dates of future hurricane landfall may affect the probabilities of coastal change. We assume that dune elevations change relatively slowly under non-storm conditions. Changes in beach slope, which will in turn affect the elevation of wave runup, may occur much more frequently, as the foreshore profile adjusts to the daily wave climate. However, use of a mean beach slope (fig. 7) in this analysis provides a more temporally stable estimate of slope and hence a more consistent measure of storm-induced wave runup.

4.2 Relative importance of waves and storm surge

Hurricane-induced coastal changes are due to waves and surge and the interaction of these processes with coastal morphology. Waves (setup and swash) were shown to increase water levels at the shoreline by 170 percent for a category 1 storm when compared to considering storm surge alone. Using a gulf-wide average of wave height and period for a category 1 hurricane (table 2), the predicted wave-driven component of shoreline water levels, η_{R2}, was 2.8 m, high enough to overwash the mean dune elevation (z_c = 2.4), even without surge. For the category 2 conditions modeled in this analysis, the wave-driven and storm surge components were of equal magnitudes. During a category 5 storm, the magnitude of surge was almost double that of wave component; however, the magnitude of runup was over 3 m, exceeding the mean dune crest height and significant enough to determine the vulnerability of the highest dunes.

The importance of waves in the lower strength wind categories, and the vulnerability of the entire basin to a category 1 storm, suggests that the impacts of less extreme weather events are likely to be significant and, under these conditions, waves may play a more important role than storm surge. Tropical storms and cold fronts in the gulf can provide the energy to significantly erode beaches and dunes. Waves during tropical storms can reach 5 m in height with wave periods of 12 s. Given these input conditions and a mean beach slope of 0.03, water levels (η_{R2}, = 1.63) would be high enough to force dune erosion over large portions of the basin (μz_t = 1.6 m). In fact, along much of the Louisiana coastline and in parts of west-central Florida, very low beaches would be vulnerable to overwash during these less extreme conditions (fig. 17; table 1).

4.3 Assessment updates

The vulnerability of sandy beaches can be expected to change in the future due to variations in storminess, sea-level rise, and human engineering efforts that alter beach configurations. As new observations and storm predictions become available, this assessment will be revised to provide updated probabilities as well as a synthesis of how coastal vulnerability to storms changes in the future (*http://coastal.er.usgs.gov/hurricanes/erosionhazards/gom*). Specifically, coastal topography will be updated to account for actual storm-driven, or even engineered, changes to the coast associated with hurricane recovery, coastal restoration, and mitigation. This updating process is underway nearly continuously as USGS, USACE, State agencies, and other entities utilize increasingly effective lidar capabilities in acquiring coastal coverage for a variety of surveying needs. Examples of these updates associated with major hurricane landfall can be found at *http://coastal.er.usgs.gov/hurricanes/*. Furthermore, as modeling develops, such as improvements to include storm size (Irish and others, 2008), surge inputs to coastal change analyses will be updated accordingly.

5. Conclusion

This assessment quantifies the probabilities of dune erosion, dune overwash, and beach/dune inundation during the landfall of category 1-5 hurricanes. The probabilities were calculated by comparing beach/dune elevations to modeled estimates of the hurricane-induced total water level at the shoreline, including contributions from both waves and storm surge. The beaches, coastal infrastructure, and habitat of the Gulf of Mexico are vulnerable to extreme coastal changes during landfall of even category 1 hurricanes. The severity of these changes increases as the intensity of the storm-driven surge and waves increases and as the height of protective dunes decreases. Citizens and coastal managers who need to

understand, plan for, and adapt to different levels of vulnerability will benefit from guidance on the likelihood of encountering mild, moderate, or severe erosion associated with different storm intensities.

By including wave-driven setup and swash in addition to storm surge, we have identified the relative importance of waves in terms of their impact on erosion vulnerability. For category 1 to 3 hurricanes, wave runup is of greater or equal magnitude as storms surge. As storm intensity increases, the relative importance of storm surge grows at a fast rate as nearshore wave height is limited due to dissipation by white-capping and breaking. Analyses that ignore the wave component of this problem will underestimate erosion vulnerability, particularly for lower category storms (or even weak tropical storms or cold fronts) .

The combination of large waves and surges and low coastal elevations makes the entire gulf region vulnerable to significant coastal erosion during storms. For a category 1 hurricane direct landfall, 99 percent of dune-backed beaches in the Gulf of Mexico are very likely (p>90 percent) to experience dune erosion during the collision regime. Overwash during a category 1 landfall is very likely along 71 percent of the coast. For wave and surge conditions representative of a category 3 hurricane, 92 percent of the Gulf of Mexico coastal areas are very likely to experience overwash and associated erosion. During category 5 conditions, 89 percent of the Gulf of Mexico beaches and dunes are very likely to be vulnerable to erosion due to inundation. The morphologic impacts from frequent and intense tropical storm events have increased the vulnerability of the Gulf of Mexico region to impacts from less extreme events in the future.

6. Acknowledgments

The USGS National Assessment of Coastal Change Hazards Project Extreme Storms and Hurricanes group thanks the many scientists and research assistants who have contributed to the research

and data collections that made this assessment possible: Katy Serafin, Laura Fauver, Peter Howd, Joe Long, Kristy Guy, Karen Morgan, Brendan Dwyer, Jolene Gittens, Bryan McCloskey, and Rob Wertz. We also thank the EAARL and CHARTS programs as well as USGS field support and survey teams for the comprehensive lidar data set that formed the basis of this analysis. Erika Lentz and Jamie Cormier provided thorough and thoughtful reviews. This research has been supported by the USGS Coastal and Marine Geology Program.

References Cited

Doran, K.S., Plant, N.G., Stockdon, H.F., Sallenger Jr., A.H., and Serafin, K.A., 2009a, Hurricane Ike: Observations and analysis of coastal change: U.S. Geological Survey Open-File Report 2009-1061, 35 p, available at http://pubs.usgs.gov/of/2009/1061/.

Doran, K.S., Stockdon, H.F., Plant, N.G., Sallenger Jr., A.H., Guy, K., and Serafin, K.A., 2009b, Hurricane Gustav: Observations and analysis of coastal change: U.S. Geological Survey Open-File Report 2009-1279, 28 p, available at http://pubs.usgs.gov/of/2009/1279/.

Holthuijsen, L.H., Booij, N., and Ris, R.C., 1993, A spectral wave model for the coastal zone, in 2nd International Symposium on Ocean Wave Measurement and Analysis, New Orleans, Louisiana, p. 630-641.

Houston, S.H., Shaffer, W.A., Powell, M.D., and Chen, J., 1999, Comparisons of HRD and SLOSH surface wind fields in hurricanes: Implications for storm surge modeling: Weather and Forecasting, v. 14, p. 671-686.

Irish, J.L., Resio, D.T., and Cialone, M.A., 2009, A surge response function approach to coastal hazard assessment. Part 2: Quantification of spatial attributes of response functions: Natural Hazards, v. 51, no. 1, p. 183-205.

Irish, J.L., Resio, D.T., and Ratcliff, J.J., 2008, The influence of storm size on hurricane surge: Journal of Physical Oceanography, v. 38, no. 9, p. 2003-2013.

Jarvinen, B.R., and Lawrence, M.B., 1985, An evaluation of the SLOSH storm surge model: Bulletin of the American Meteorological Society, v. 66, no. 11, p. 1408-1411.

Le Treut, H., Somerville, R., Cubasch, U., Ding, Y., Mauritzen, C., Mokssit, A., Peterson, T., and Prather, M., 2007, Historical overview of climate change, *in* Climate Change 2007: The Physical Science Basis: Cambridge University Press, Cambridge.

National Oceanic and Atmospheric Administration (NOAA), 2007, Hurricane preparedness: SLOSH model, National Hurricane Center.

Plant, N.G., Holland, K.T., and Puleo, J.A., 2002, Analysis of the scale of errors in nearshore bathymetric data: Marine Geology, v. 191, no. 1-2, p. 71-86.

Plant, N.G., and Stockdon, H.F., in press, Probabilistic prediction of barrier-island response to hurricanes: Journal of Geophysical Research Earth Surface.

Plant, N.G., Stockdon, H.F., Sallenger Jr., A.H., Turco, M.J., East, J.W., Taylor, A.A., and Shaffer, W.A., 2010, Forecasting hurricane impact on coastal topography: Eos Transactions American Geophysical Union, v. 91, no. 7, p. 65-66.

Ruggiero, P., and List, J.H., 2009, Improving accuracy and statistical reliability of shoreline position and change rate estimates: Journal of Coastal Research, v. 25, no. 5, p. 1069-1081.

Sallenger, A.H., 2000, Storm impact scale for barrier islands: Journal of Coastal Research, v. 16, no. 3, p. 890-895.

Sallenger, A.H., Krabill, W., Swift, R., Brock, J., List, J., Hansen, M., Holman, R.A., Manizade, S., Sontag, J., Meredith, A., Morgan, K., and Stockdon, H., 2003, Evaluation of airborne scanning lidar for coastal change applications: Journal of Coastal Research, v. 19, p. 125-133.

Sallenger, A.H., Stockdon, H.F., Fauver, L.A., Hansen, M., Thompson, D.T., Wright, C.W., and Lillycrop, J., 2006, Hurricanes 2004: An overview of their characteristics and coastal change: Estuaries and Coasts, v. 29, no. 6A, p. 880-888.

Stockdon, H.F., Doran, K.S., and Sallenger, A.H., 2009, Extraction of lidar-based dune-crest elevations for use in examining the vulnerability of beaches to inundation during hurricanes: Journal of Coastal Research, v. 25, no. 6, p. 59-65.

Stockdon, H.F., Holman, R.A., Howd, P.A., and Sallenger, A.H., 2006, Empirical parameterization of setup, swash, and runup: Coastal Engineering, v. 53, no. 7, p. 573-588.

Stockdon, H.F., Sallenger, A.H., Holman, R.A., and Howd, P.A., 2007a, A simple model for the spatially-variable coastal response to hurricanes: Marine Geology, v. 238, p. 1-20.

Stockdon, H.F., Thompson, D.M., and Sallenger, A.H., 2007b, Hindcasting potential hurricane impacts on rapidly changing barrier islands, *in* Proceedings, Coastal Sediments '07:Sixth International Symposium on Coastal Engineering and Science of Coastal Sediment Processes, New Orleans, La., May 13-17, 2007, American Society of Civil Engineers, p. 976-985.

Weber, K.M., List, J.H., and Morgan, K.L.M., 2005, An operational mean high water datum for determination of shoreline position from topographic lidar data: U.S. Geological Survey Open-File Report 2005-1027, available at http://pubs.usgs.gov/of/2005/1027/.

Tables

Table 1. Mean elevation of dune crest (z_c) and dune toe (z_t) and mean beach slope (β_m) for the sandy beaches along the Gulf of Mexico coast. [Standard deviation is given in parenthesis. m, meter]

State/region	z_c(m)	z_t (m)	β_m	Survey date (month/year)
U.S. Gulf of Mexico	2.43 (1.02)	1.06 (0.59)	0.032 (0.021)	
Texas	2.72 (1.50)	1.84 (0.88)	0.033 (0.026)	8/2000, 9/2005,9/2008
Louisiana	1.57 (0.64)	1.33 (0.37)	0.020 (0.014)	9/2005, 3/2008, 9/2008
Mississippi	2.24 (0.70)	1.34 (0.46)	0.016 (0.009)	6/2007, 9/2008
Alabama	3.05 (0.87)	1.93 (0.68)	0.038 (0.019)	9/2008
Florida Panhandle	3.18 (1.69)	1.85 (0.80)	0.039 (0.022)	6/2008, 9/2008
Florida west coast	1.84 (0.74)	1.32 (0.35)	0.047 (0.033)	11/2004, 5/2006

Table 2. Mean input wind speed, significant wave height (H_s), and wave period (T_p) and modeled setup (η_{setup}), runup (η_{R2}) and storm surge (η_{surge}) for category 1-5 hurricanes. [Standard deviation is given in parenthesis. m, meter; m/s, meters per second; s, second]

Hurricane intensity category	Wind speed (m/s)	H_s(m)	T_p (s)	η_{setup} (m)	η_{R2} (m)	η_{surge} (m)
1	42.5	7.58 (0.14)	16.85 (0.64)	0.69 (0.37)	2.86 (0.64)	1.68 (0.28)
2	49.2	7.83 (0.11)	17.22 (0.60)	0.71 (0.38)	2.98 (0.65)	2.86 (0.45)
3	58.1	8.18 (0.08)	17.75 (0.57)	0.75 (0.40)	3.14 (0.67)	3.96 (0.59)
4	69.3	8.62 (0.06)	18.42 (0.60)	0.80 (0.42)	3.34 (0.71)	5.01 (0.70)
5	73.8	8.79 (0.06)	18.68 (0.62)	0.82 (0.43)	3.42 (0.73)	6.02 (0.79)

Table 3. Percent of coast very likely (p>0.9) to experience erosion associated with collision, overwash, and inundation during category 1-5 hurricanes.

	Hurricane intensity category				
	1	2	3	4	5
Collision					
U.S. Gulf of Mexico	99	100	100	100	100
Texas	99	100	100	100	100
Louisiana	100	99	100	100	100
Mississippi	100	100	100	100	100
Alabama	100	100	100	100	100
Florida Panhandle	98	99	100	100	100
Florida west coast	99	100	100	100	100
Overwash					
U.S. Gulf of Mexico	71	85	92	97	98
Texas	61	75	88	98	99
Louisiana	95	99	100	100	100
Mississippi	96	100	100	100	100
Alabama	69	99	100	100	100
Florida Panhandle	47	74	83	89	93
Florida west coast	98	99	100	100	100
Inundation					
U.S. Gulf of Mexico	27	58	73	83	89
Texas	20	54	62	73	85
Louisiana	62	86	95	100	100
Mississippi	35	93	100	100	100
Alabama	4	29	74	99	100
Florida Panhandle	5	25	51	69	77
Florida west coast	42	91	99	99	99